



## Glycerol Oligomerization Using Low Cost Dolomite Catalyst

Fernando José S. Barros<sup>1</sup> · Juan A. Cecilia<sup>2</sup> · Ramón Moreno-Tost<sup>2</sup> · Matheus F. de Oliveira<sup>1</sup> · Enrique Rodríguez-Castellón<sup>2</sup> · Francisco Murilo T. Luna<sup>1</sup> · Rodrigo S. Vieira<sup>1</sup>

Received: 15 May 2018 / Accepted: 27 September 2018  
© Springer Nature B.V. 2018

### Abstract

Production of glycerol oligomers by heterogeneous catalysis is being studied as an option for valorization of this biodiesel by-product. In this study, the catalytic activity of dolomite and the effects of parameters such as catalyst loading, reaction temperature, and reaction time were evaluated. Reusability and stability test were also performed. The material was tested as-received and after a thermal treatment, being characterized by XRD, FTIR, N<sub>2</sub> adsorption–desorption, SEM, CO<sub>2</sub>-TPD and TG/DTG. Reaction products were analyzed by GC-FID for oligomers composition and ICP to verify metallic species leaching. The thermal treatment led to a decrease of the particle size, increase of the specific surface area and improved basicity. Calcined dolomite showed better catalytic performance than natural dolomite, leading to almost 80% glycerol conversion and selectivities for diglycerol and triglycerol of 51% and 3%, respectively. Kinetic test revealed that the reaction is slow along the first hours and later the reaction rate increases. Ca and Mg are leached to the reaction medium but the catalyst could be reused up to 2 cycles, with similar diglycerol yield. The reaction conditions for this material are less severe than those reported previously, which added to the low cost and reusability capacity turns suitable for glycerol oligomerization process.

### Graphical Abstract



**Keywords** Glycerol · Etherification · Dolomite · Diglycerol · Triglycerol

### Statement of Novelty

To the best of our knowledge, a profound study including the characterization and evaluation of dolomite as catalyst for valorization of glycerol, a by-product of biodiesel industry, in oligoglycerols has not been addressed yet. The change from a homogeneous industrial catalytic process to

✉ Rodrigo S. Vieira  
rodrigo@gpsa.ufc.br

Extended author information available on the last page of the article

29 a heterogeneous one will turn it into more sustainable one.  
30 Moreover, the abundancy, worldwide distribution and the  
31 low cost of dolomites are important features to make it also  
32 economically viable. In this manuscript, the influence of  
33 both basicity and textural properties will be evaluated in the  
34 reaction. The thermally modified solid showed good activity  
35 and reusability, under reaction conditions lower than those  
36 reported for commercial catalysts, what are interesting fea-  
37 tures for the development of a new process.

## 38 Introduction

39 Several energy sources have been proposed to gradually  
40 replace the traditional fossil fuels. Among them, the use of  
41 biomass seems to be a sustainable source to obtain chemicals  
42 and fuel through catalytic processes. In the last decades,  
43 the synthesis of biodiesel from vegetable oils, like soybean  
44 oil, palm oil, etc., and short-chain alcohols has gained wide  
45 interest as alternative fuel [1].

46 The synthesis of biodiesel also forms glycerol as by-pro-  
47 duct. The increasing production of this fuel worldwide has  
48 led to a surplus of glycerol, causing a decrease in the price.  
49 In fact, glycerol was initially discarded or stored without  
50 specific purposed [2]. This compound is a colorless, viscous,  
51 and non-toxic liquid, which is frequently used in the food,  
52 cosmetics, soaps and toothpastes, sweetener and pharmaceu-  
53 tical industries [2–4]. The presence of three hydroxyl groups  
54 provides to its molecule a diverse reactivity to obtain a large  
55 amount of valuable compounds by diverse chemicals reac-  
56 tions. Therefore, one major challenge on this topic is to find  
57 a way to take advantage of glycerol potential, enhancing its  
58 market value through low-cost chemical routes [5].

59 Thus, the glycerol conversion into high-added value prod-  
60 ucts by dehydration to obtain acrolein has been reported in  
61 the literature [6, 7], hydrogenolysis to obtain propanediols  
62 [8], oxidation [9, 10] as well as conversion to syngas [11] or  
63 the synthesis of fatty esters [12]. The glycerol etherification  
64 is another reaction to valorize this by-product obtained in  
65 the biodiesel industry. Previous authors have carried out the  
66 glycerol etherification with alkenes [13], with other alcohols  
67 [14] or even solventless [15–17].

68 Glycerol can react with itself to form short-chain oligom-  
69 ers (di- and triglycerol). The production of those compounds  
70 has motivated the scientific community due to its wide range  
71 of applications, such as in cosmetics, polymers, food addi-  
72 tives, plastic coating industry, biomedical and drug admin-  
73 istration systems [18]. One feature that has made increase  
74 the interest for these compounds is their potential to replace  
75 petrochemical-based glycol, used as coalescent in paints,  
76 solvents, and inks or in cleaning formulations, however,  
77 some of them are toxic such as short ethylene glycols [19].  
78 On cosmetic applications, diglycerol is used to enhance

79 fragrance, flavor impact and longevity in products such as  
80 toothpastes, mouthwashes and deodorant sticks [20]. Di- or  
81 triesters of glycerol oligomers can be synthesized via ester-  
82 ification with carboxylic acids or transesterification with car-  
83 boxylic acid methyl esters [3]. Previous works have reported  
84 that lower amounts of diglycerol monooleate can achieve an  
85 antifogging effect in food packages [21].

86 The glycerol oligomerization reaction has been  
87 approached from homogenous catalysis point of view, using  
88 both acid and basic catalysts such as  $H_2SO_4$  and  $CsHCO_3$   
89 [22, 23]. The use of heterogeneous catalysts has emerged as  
90 alternative to the traditional homogenous catalysts since the  
91 heterogeneous catalysts can be easier purified and reused.  
92 Several solid acid catalysts, such as cationic exchange res-  
93 ins and zeolites have shown activity in solventless glycerol  
94 etherification [20, 24, 25]. The use of heterogeneous base  
95 catalysts is also reported in this reaction. Thus, Ruppert  
96 et al. [26] evaluated the use of different alkaline-earth metal  
97 oxides (MgO, CaO, SrO and BaO) in the glycerol etherifi-  
98 cation, establishing that the glycerol conversion is closely  
99 related with the strength of the basic sites of the catalysts.  
100 In this sense, Barros et al. [17] used eggshell as natural and  
101 inexpensive source as catalytic precursor to obtain CaO  
102 with high activity in the glycerol etherification reaction. In  
103 the same way, Clacens et al. [27] using  $Cs^+$  as active phase  
104 supported on silica MCM-41 to disperse the active phase,  
105 achieved a good activity and selectivity. In addition, these  
106 authors reported that an increase of the glycerol conversion  
107 also leads to a loss of the selectivity towards di- and tri-  
108 glycerols. Recently, layered double hydroxides (LDHs) have  
109 been used as catalytic precursors to obtain mixed-oxides cat-  
110 alysts ( $MgO-Al_2O_3$ ,  $CaO-Al_2O_3$  and  $MgO-Fe_2O_3$ ), which  
111 display high specific surface area and high availability of  
112 active sites [15, 16, 28].

113 Considering that solid basic catalysts with high basic-  
114 ity have reached interesting yields to di- and triglycerols,  
115 dolomite could be considered a natural source with high  
116 potential to obtain solid basic catalysts after a thermal treat-  
117 ment. This double carbonate of calcium and magnesium  
118 ( $CaCO_3 \cdot MgCO_3$ ) is a recurring mineral in the nature, formed  
119 by dolomitization process from magnesium substitution on  
120 calcite, and has a theoretical content of 45.7%  $MgCO_3$  and  
121 54.3% of  $CaCO_3$ . Dolomite has found different applications,  
122 such as a refractory material, as well as a fluxing agent in  
123 metallurgical, glass and ceramic industry; and filling mate-  
124 rial in paper, rubber and plastic production. Large amounts  
125 of dolomite are also used in building industry and agricul-  
126 ture [29].

127 In addition, this material has been used as precursor  
128 in several catalytic processes such as the production of  
129 biodiesel from canola or sunflower oil with short-chain  
130 alcohols, achieving excellent conversion rates in all cases  
131 [30–32]. Dolomite was used as catalyst in the reaction

132 between glycerol and dimethyl carbonated (DMC) to obtain  
133 glycerol carbonate, reaching a glycerol conversion of 97%  
134 and glycerol carbonate yield of 94% [33]. The material has  
135 also been tested as catalytic support in Ni/dolomite catalysts  
136 in the H<sub>2</sub> production from the pyrolysis gasification of waste  
137 tires, achieving a yield of 49.1% [34].

138 The aim of this research is the use of dolomite as catalytic  
139 precursor in the glycerol etherification without solvent. For  
140 this purpose, dolomite is thermally activated to obtain their  
141 respective metal oxides (CaO–MgO), considered as active  
142 phase in the etherification reaction. The present research  
143 evaluates the influence of catalyst loading, temperature and  
144 reaction time. In addition, the stability and reusability tests  
145 have been also performed with the catalyst with the highest  
146 yield under the best catalytic conditions.

## 147 Experimental Section

### 148 Catalysts Preparation

149 Dolomite was provided by a local industry (Itamil Itaoca),  
150 the as-received sample was labeled as ND (natural dolo-  
151omite). The material was activated by calcination at 800 °C  
152 for 2 h in a muffle furnace (EDG equipment), being labeled  
153 as CD (calcined dolomite). The activation conditions were  
154 chosen considering previous research on calcium natural  
155 sources [31].

### 156 Catalyst Characterization

157 The chemical composition was measured with an X-ray fluo-  
158rescence spectrometer Rigaku brand, model ZSX mini II,  
159 operating at a voltage of 40 kV and a current of 1.2 mA in  
160 the tube coupled to Pd.

161 The crystalline phases of natural and calcined dolo-  
162omite were determined by X-ray diffraction (XRD) using  
163 an X'Pert Pro MPD diffractometer with Co K $\alpha$  radiation  
164 ( $\lambda = 1.788965 \text{ \AA}$ ) operating at a voltage of 40 kV and a cur-  
165rent of 40 mA. To perform the analysis, sample powders  
166 were placed in the cavity of the support used as the sample  
167 holder. The diffractograms were obtained by sweeping in the  
168 range 10–70° at a scan rate of 0.5 min<sup>-1</sup>.

169 Thermal decomposition of the catalysts was evaluated  
170 by thermogravimetric analysis/differential thermal analy-  
171sis (TG/DTG), carried out on a STA 449 F3-JUPITER/  
172NETZSCH analyzer operating under the following condi-  
173tions: flow N<sub>2</sub> (50 mL min<sup>-1</sup>); heating rate, 10 °C min<sup>-1</sup>;  
174 temperature, from room temperature 40–1000 °C.

175 FTIR was used to follow the functional group transforma-  
176tion during the thermal process on dolomite (IR-PRESTIGE  
17721 SHIMADZU FTIR). Samples were analyzed in the range  
178 of 400–4000 cm<sup>-1</sup>, with spectral resolution of 4.0 cm<sup>-1</sup>. The

179 textural analyses of catalysts were performed with Autosorb  
180 1-MP equipment (Quantachrome Instruments). The nitro-  
181gen adsorption–desorption measurements were carried out  
182 at –196 °C with a sample previously treated at 300 °C for  
183 12 h with N<sub>2</sub>. Pore diameter and pore volume were deter-  
184 mined from the adsorption branch of the isotherms by the  
185 Barrett–Joyner–Hallenda (BJH) method. The surface area  
186 was determined according to the Brunauer–Emmett–Teller  
187 (BET) method (S<sub>BET</sub>).

188 The surface morphology of precursor and catalyst was  
189 observed using a JEOL JXA-840A scanning electron micro-  
190 scope (20 kV) under a vacuum of 1.33 × 10<sup>-6</sup> mbar (Jeol,  
191 Japan), both samples were initially covered with a thin layer  
192 of gold (10 nm) using a sputter coater (SCD 050; Baltec,  
193 Liechtenstein).

194 The basicity of the calcined dolomite was studied by  
195 temperature-programmed desorption of CO<sub>2</sub>, where approx-  
196 imately 100 mg of sample was pretreated in helium flow  
197 (60 mL min<sup>-1</sup>) at 800 °C for 30 min (10 °C min<sup>-1</sup>). The  
198 reaction temperature was lowered to 100 °C and pure CO<sub>2</sub>  
199 stream (60 mL min<sup>-1</sup>) was subsequently introduced into the  
200 reactor for 30 min. The reaction of CO<sub>2</sub>-TPD was conducted  
201 between 100 and 800 °C helium flow (10 °C min<sup>-1</sup> and  
202 30 mL min<sup>-1</sup>) and the amount of CO<sub>2</sub> evolved was analyzed  
203 using a quadrupole mass spectrometer (Balzer 02 GSB 200)  
204 equipped with a Faraday detector (0–200 U) that monitored  
205 the weight of CO<sub>2</sub> (44 U) during the experiment.

### 206 Reaction Procedure

207 Glycerol etherification was carried out in batch reactor (Parr  
208 model), using 100 g of glycerol under nitrogen flow. First,  
209 the reactor was loaded with glycerol and the temperature was  
210 raised up to the set point, then the catalyst was added under  
211 nitrogen flow and this time was considered as time zero. The  
212 reactions were carried out in a range of temperature between  
213 200 and 245 °C, with catalyst loading of 0.5–2 wt% for 24 h.

214 Kinetic reaction was accomplished and monitored at the  
215 intervals of time of 1, 2, 3, 4, 5, 6 and 24 h, the test was  
216 started when the temperature of the reactor was stabilized.  
217 Sampling occurred through a tube inserted into the middle  
218 of the reaction medium and a valve allowed the withdrawal  
219 of aliquots during the reaction without opening the reactor.

220 For the first reusability study, the catalyst was separated  
221 from the mixture of reaction by decantation. Then, the  
222 recovered solid was used on the next test, carried out in the  
223 same reaction conditions. On the second set of tests, the  
224 catalyst was separated of the reaction medium by vacuum  
225 filtration on a porous plate after being diluted on deionized  
226 water, finally, the recovered solid was calcined at 800 °C for  
227 2 h prior the new reaction cycle.

228 The reaction medium was analyzed by means of gas  
229 chromatography with a flame ionization detector GC-FID

230 (Agilent) following the same methodology for products  
 231 silylation with BSTFA as well analysis of reaction param-  
 232 eters reported on Barros et al. [17] in terms of glycerol con-  
 233 version ( $X_{\text{gly}}$ ), selectivities for diglycerol ( $S_{\text{di}}$ ), triglycerol  
 234 ( $S_{\text{tri}}$ ), high oligomers and other products ( $S_{\text{ho}}$ ) and oligomers  
 235 yielding ( $Y_{\text{di}}$  and  $Y_{\text{tri}}$ ).

236 The determination of Ca leaching in the reaction medium  
 237 was carried out by ICP using an ICP-OES (Thermo Fisher  
 238 Scientific—Model iCAP 6000) equipment. Reaction mixture  
 239 and catalyst were separated by filtration; 1 mg of sample  
 240 was diluted on 10 mL of ultrapure water and then filtrated  
 241 through a syringe filter with a pore diameter of 0.45  $\mu\text{m}$ . A  
 242 calibration curve was prepared by using an aqueous multi-  
 243 elemental standard solution of Ca and Mg.

## 244 Results and Discussion

### 245 Dolomite Characterization

246 The chemical composition of dolomite was determined by  
 247 X-ray fluorescence (XRF) (Table 1). Taking into account  
 248 that several elements such as carbon and oxygen, which  
 249 are present in dolomite, cannot be determined by XRF, the  
 250 data reveal that dolomite is mainly composed by calcium  
 251 (81.28%) and magnesium (15.30%), with minor proportions  
 252 of iron and silicon species. These data also show that the  
 253 substitution of  $\text{Ca}^{2+}$  by  $\text{Mg}^{2+}$  species is relatively low. As it  
 254 was expected, the thermal activation does not cause signifi-  
 255 cant changes in the elemental composition of the material.

256 Figure 1 shows Thermo-XRD patterns of dolomite. The  
 257 experiment started with natural dolomite (ND) at 30  $^{\circ}\text{C}$ .  
 258 The material exhibited the characteristic peaks of tremo-  
 259 lite, a member of the calcic amphibole group of silicate  
 260 minerals with the chemical formula  $\text{Ca}_2\text{Mg}_5\text{Si}_8\text{O}_{22}(\text{OH})_2$ .  
 261 From 100 to 600  $^{\circ}\text{C}$ , the solid exhibited peaks at  $2\theta = 29.6$   
 262 and  $30.9^{\circ}$ . Less intense peaks between  $35\text{--}55^{\circ}$  are consist-  
 263 ent with dolomite ( $33.28, 35.37, 41^{\circ}, 43.75, 44.86, 50.25,$   
 264 and  $50.79^{\circ}$ ). At 700  $^{\circ}\text{C}$ , the peaks ascribed to  $\text{CaCO}_3$  and  
 265 MgO increased their intensity and also the shrinkage of  
 266 dolomite peaks takes place, even after that, some dolomite  
 267 phase still remains, in accordance with results observed  
 268 by Engler et al. [35]. At 800  $^{\circ}\text{C}$ , the characteristic peaks  
 269 ascribed to dolomite and calcite decrease in intensity and  
 270 new crystalline phases arise which can be attributed to

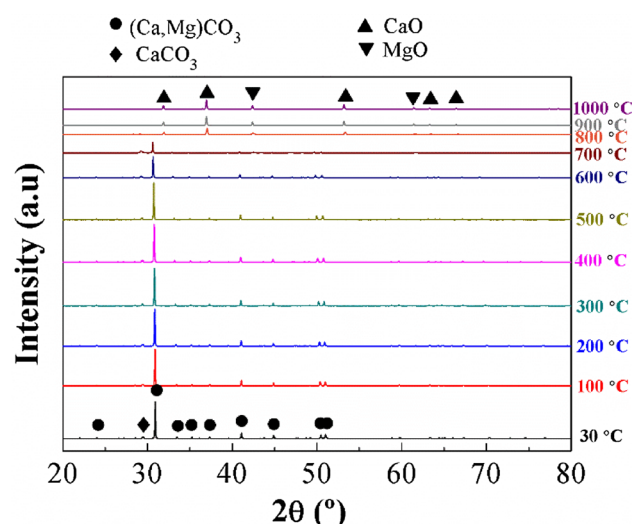


Fig. 1 Thermo-X-ray diffraction of natural dolomite

271 MgO ( $48.47^{\circ}$ ) and CaO ( $32$  and  $38^{\circ}$ ), in agreement with  
 272 the findings reported by Shahraki et al. [29]. Moreover,  
 273 reflection peaks ascribed to  $\text{CaCO}_3$  ( $37$  and  $42.5^{\circ}$ ) can  
 274 be still observed. Finally, at 900  $^{\circ}\text{C}$ ,  $\text{CaCO}_3$  is still detected  
 275 and the crystallinity of both MgO and CaO phase is  
 276 slightly increased [35].

277 The crystal size was determined using the Scherrer's  
 278 equation from the main diffraction peak of each crystallo-  
 279 graphic phase. These data reveals that dolomite displays a  
 280 crystal size of 297 nm, while calcite exhibits a crystal size of  
 281 153 nm. After the thermal treatment, it is obtained lime and  
 282 periclase with a crystal size of 134 and 58 nm, respectively.

283 The thermal analysis of the natural dolomite is shown  
 284 in Fig. 2. The TG curve of the raw dolomite hardly suf-  
 285 fers mass loss below 650  $^{\circ}\text{C}$ , only 1.49%. From these  
 286 temperatures the DTG curve shows an endothermic event  
 287 between 650 and 840  $^{\circ}\text{C}$ , in which the sample displays a  
 288 mass loss of 42.28 wt%, being attributed to the decomposi-  
 289 tion of the carbonate species. These data are in agreement  
 290 with those obtained by thermo-XRD where the diffrac-  
 291 tion peaks attributed to carbonate species decrease from  
 292 600  $^{\circ}\text{C}$ . The obtained values in the decarbonation step are  
 293 close to the theoretical value of the dolomite decomposition  
 294 (47.7 wt%). The small differences could be attributed  
 295 to the presence of impurities in the natural dolomite, as  
 296 indicated the XRF data (Table 1).

Table 1 XRF data and textural parameters for ND and CD

Sample	XRF (wt%)				Textural properties		
	Ca	Mg	Fe	Si	$S_{\text{BET}}$ ( $\text{m}^2 \text{g}^{-1}$ )	$V_p$ ( $\text{cm}^3 \text{g}^{-1}$ )	$D_p$ (nm)
ND	81.28	15.30	1.27	1.51	1.57	0.01	16.16
CD	80.73	16.34	1.43	1.14	37.7	0.22	23.41

ND natural dolomite, CD calcined dolomite (800  $^{\circ}\text{C}$ , 2 h)

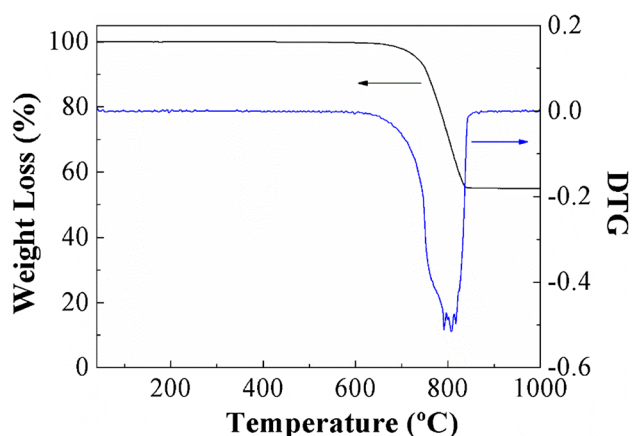


Fig. 2 TG-DTG profiles of natural dolomite

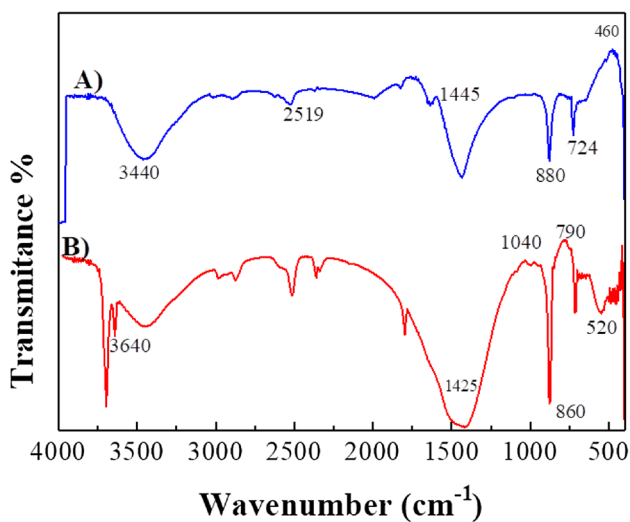


Fig. 3 Dolomite FTIR spectra a ND b CD (800 °C, 2 h)

297 The FTIR spectrum of natural dolomite (Fig. 3a) contains  
 298 the main absorption bands of dolomite: 2519, 1445, 880 and  
 299 724  $\text{cm}^{-1}$ . Sample shows intense bands relate to the presence  
 300 of absorbed water at around 3440  $\text{cm}^{-1}$ , since the material  
 301 was not thermally treated and it was analyzed as received.  
 302 A weak band due to quartz is also visible around 465  $\text{cm}^{-1}$   
 303 [29, 36]. Weak bands due to silicate phase (1040, 790, 520  
 304 and 460  $\text{cm}^{-1}$ ) are also observed, which is according to data  
 305 from X-ray fluorescence [29].

306 The CD sample shows new bands at 720, 860 and 420  $\text{cm}^{-1}$   
 307 (Fig. 3b) and the bands due to dolomite phase are missing.  
 308 These features point out the structural change from dolomite  
 309 to calcite. It must be highlighted that the CD sample was not  
 310 preserved from the atmosphere contact before FTIR analysis.  
 311 The narrow band observed at around 3640  $\text{cm}^{-1}$  and the bands  
 312 at higher wavelengths indicate that after calcination at 800 °C  
 313 the dolomite is transformed into CaO–MgO mixed oxides. The

314 presence of bands at 3640 and 1425  $\text{cm}^{-1}$  points out that the  
 315 solid is hydroxylated, giving rise the formation of  $\text{Ca}(\text{OH})_2$  in  
 316 accordance with the information obtained from XRD analysis.  
 317 According to Granados et al., the solid is hydrated very fast  
 318 during the first minutes of contacting with air [37]. The bands  
 319 at around 1425, 1074 and 860  $\text{cm}^{-1}$  can be assigned to carbon-  
 320 ate species on the surface of the CaO, indicating that the mate-  
 321 rial is readily carbonated after calcination and air exposition  
 322 [37]. There is also the appearance of a peak at 450  $\text{cm}^{-1}$  due  
 323 to the formation of MgO [29, 30].

324 The textural properties of both ND and CD are summa-  
 325 rized in Fig. 4 and Table 1. From  $\text{N}_2$  adsorption–desorption  
 326 isotherms, it can be deduced that both materials display low  
 327 porosity. Considering the IUPAC classification, the isotherms  
 328 of both ND and CD can be considered as type-II, which are  
 329 typical of macroporous materials [38]. Both materials are solid  
 330 structures without intrinsic porosity.

331 The specific surface values ( $S_{\text{BET}}$ ), reported in Table 1, are  
 332 only attributed to the  $\text{N}_2$ -filled of the interparticle voids. The  
 333 thermal treatment causes an increase of the surface area and  
 334 the pore volume. This data is in agreement with the XRD data  
 335 where the decarbonation of the dolomite leads to structures  
 336 with lower crystallinity, which generates higher proportion  
 337 of interparticle voids and porosity in comparison to the start-  
 338 ing dolomite. ND and CD pore size distribution plot shows  
 339 meso and macropores, the thermally treated material presents  
 340 a broader distribution, in accordance with previously reported  
 341 results [39, 40].

342 The morphology of ND and CD was analyzed from their  
 343 SEM images (Fig. 5). Figure 5a shows that ND displays a  
 344 smooth and irregular surface with heterogeneous particle size.  
 345 After the thermal process (Fig. 5b), the material exhibits a  
 346 greater proportion of fine particles with roughness as a conse-  
 347 quence of the exothermic process of the decarbonation, which  
 348 can even form micropores by the  $\text{CO}_2$  liberation [31].

349 The strength of the basic sites was evaluated by  $\text{CO}_2$ -TPD  
 350 (Fig. 6) from the CaO–MgO catalytic system obtained after  
 351 the thermal treatment. The graph shows the presence of two  
 352 basic sites with different strengths. The peak between 100  
 353 and 200 °C with maximum desorption near to 140 °C, can  
 354 be attributed to the interaction of  $\text{CO}_2$  with weak basic sites  
 355 associated with the oxygen in the  $\text{Mg}^{2+}\text{--O}^{2-}$  pairs [41]. The  
 356 peak located between 400 and 700 °C with maximum at about  
 357 560 °C is related to sites with strong basicity and corresponds  
 358 to basic sites ascribed to CaO. The high temperature required  
 359 to the  $\text{CO}_2$  desorption suggests the presence of strong basic  
 360 sites after the thermal activation.

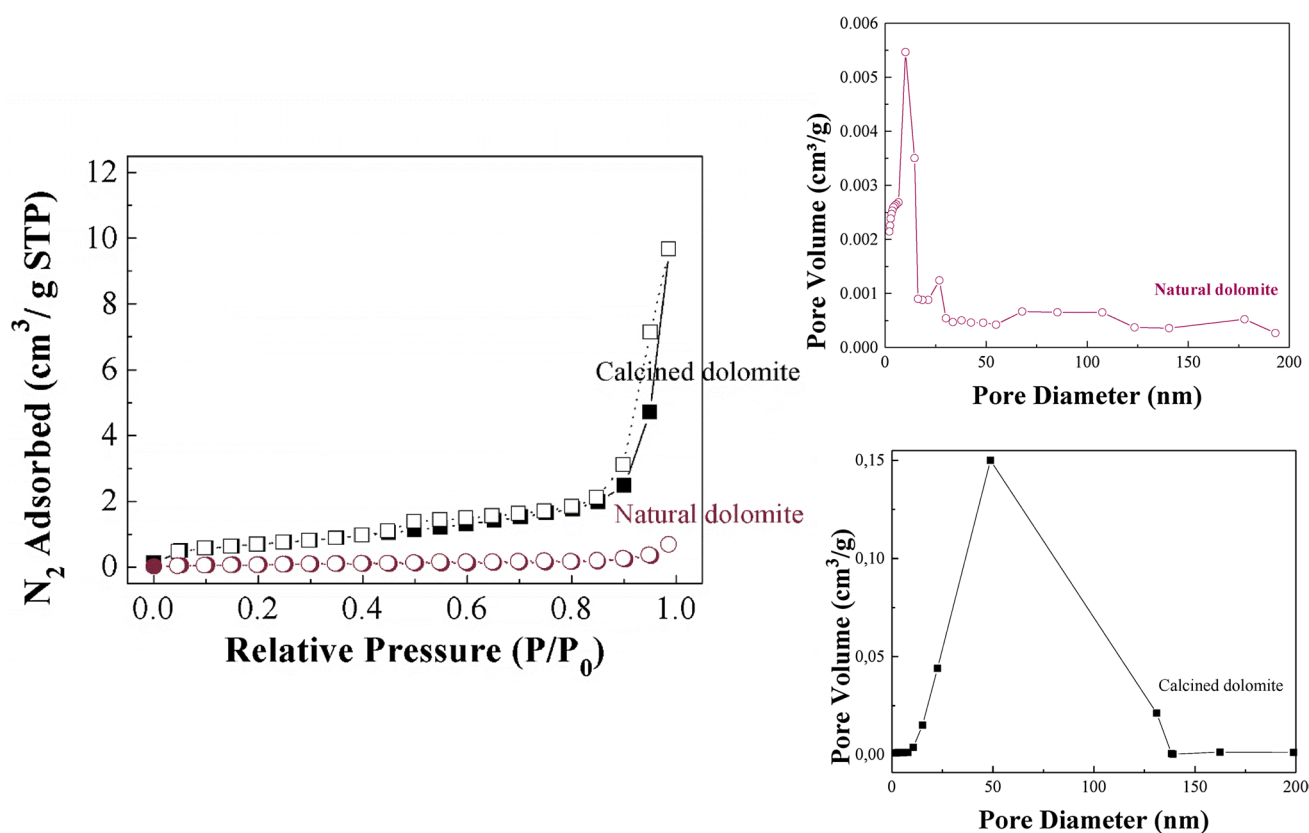


Fig. 4 Nitrogen adsorption/desorption isotherms and pore size distribution of ND and CD (800 °C, 2 h)

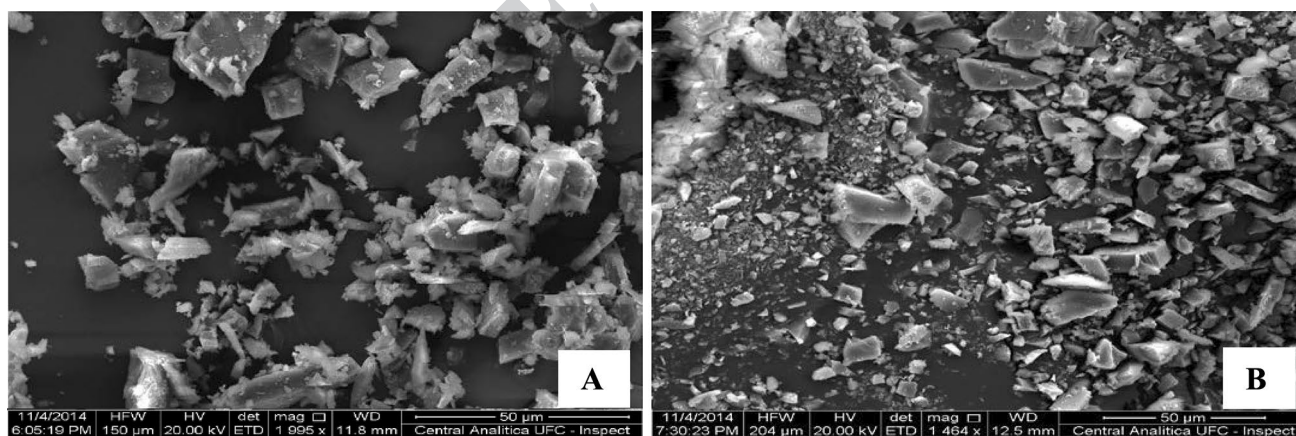


Fig. 5 SEM images a ND  $\times 1995$  b CD  $\times 1464$

## 361 Catalytic Results

### 362 Blank Test

363 In order to evaluate the promotional effect of dolomite  
 364 (Fig. 7), it was performed an experiment without catalyst  
 365 and compared with the catalytic performance of both ND or

CD catalysts. The reaction was carried out at 245 °C and 6 h  
 of time on stream and catalyst loading of 2 wt%.

It is observed that in absence of catalyst, glycerol conversion ( $X_{gly} = 23\%$ ) is similar to that with ND (22%) and lower than the one with the presence of CD (37%). Both catalysts increased diglycerol selectivity, from  $S_{di} = 29\%$  for the blank test to 52% on ND case and 55% for CD, leading the calcined

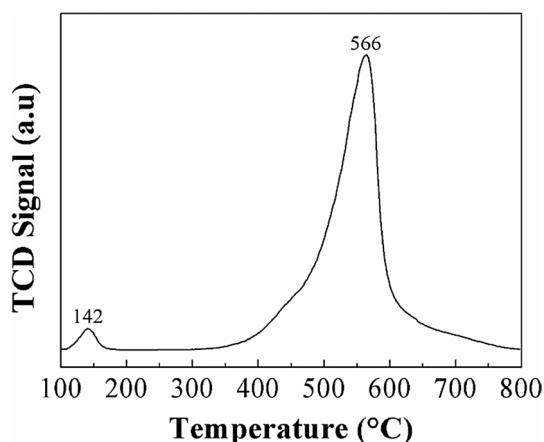


Fig. 6 CO<sub>2</sub>-TPD of the calcined dolomite at 800 °C for 2 h

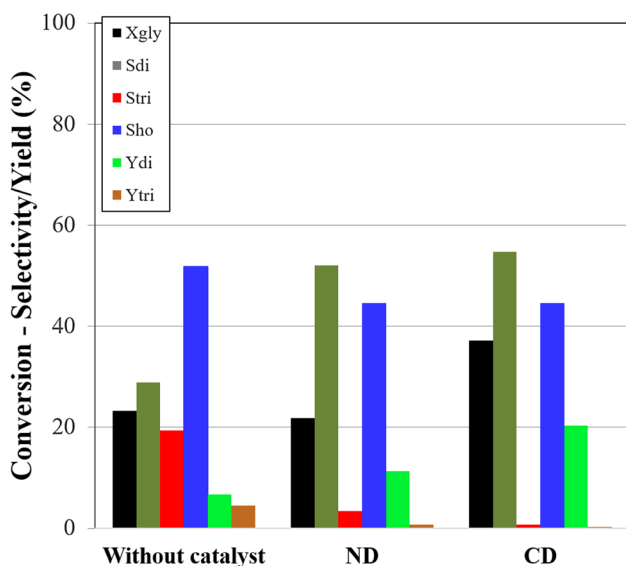
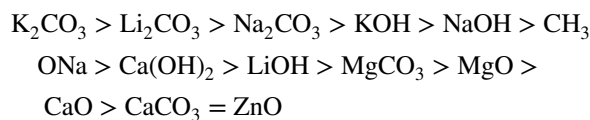


Fig. 7 Glycerol conversion ( $X_{Gly}$ ), selectivities to diglycerol ( $S_{di}$ ), triglycerol ( $S_{tri}$ ), high oligomers and other products ( $S_{ho}$ ), diglycerol yield ( $Y_{di}$ ) and triglycerol yield ( $Y_{tri}$ ) for tests without catalyst, with 2 wt% of natural dolomite and 2 wt% of calcined dolomite (reaction conditions: 245 °C, 6 h)

373 material to the highest  $Y_{di}$ , 20%. Regarding the dolomitic  
 374 material, it was observed that the activation of the catalyst  
 375 was effective in increasing the glycerol conversion as well as  
 376 diglycerol yield, reaching higher values than those obtained  
 377 without thermal treatment of the solid.

378 XRD and FTIR analysis have pointed to the presence  
 379 of CaO–MgO mixed oxides as major constituents of cal-  
 380 cined dolomite. However, XRD also confirmed that CaCO<sub>3</sub>  
 381 remains after thermal treatment. Garti et al. [42] has com-  
 382 pared several base catalysts on glycerol polymerization at  
 383 lower reaction times (4 h), finding the following order of  
 384 activity:



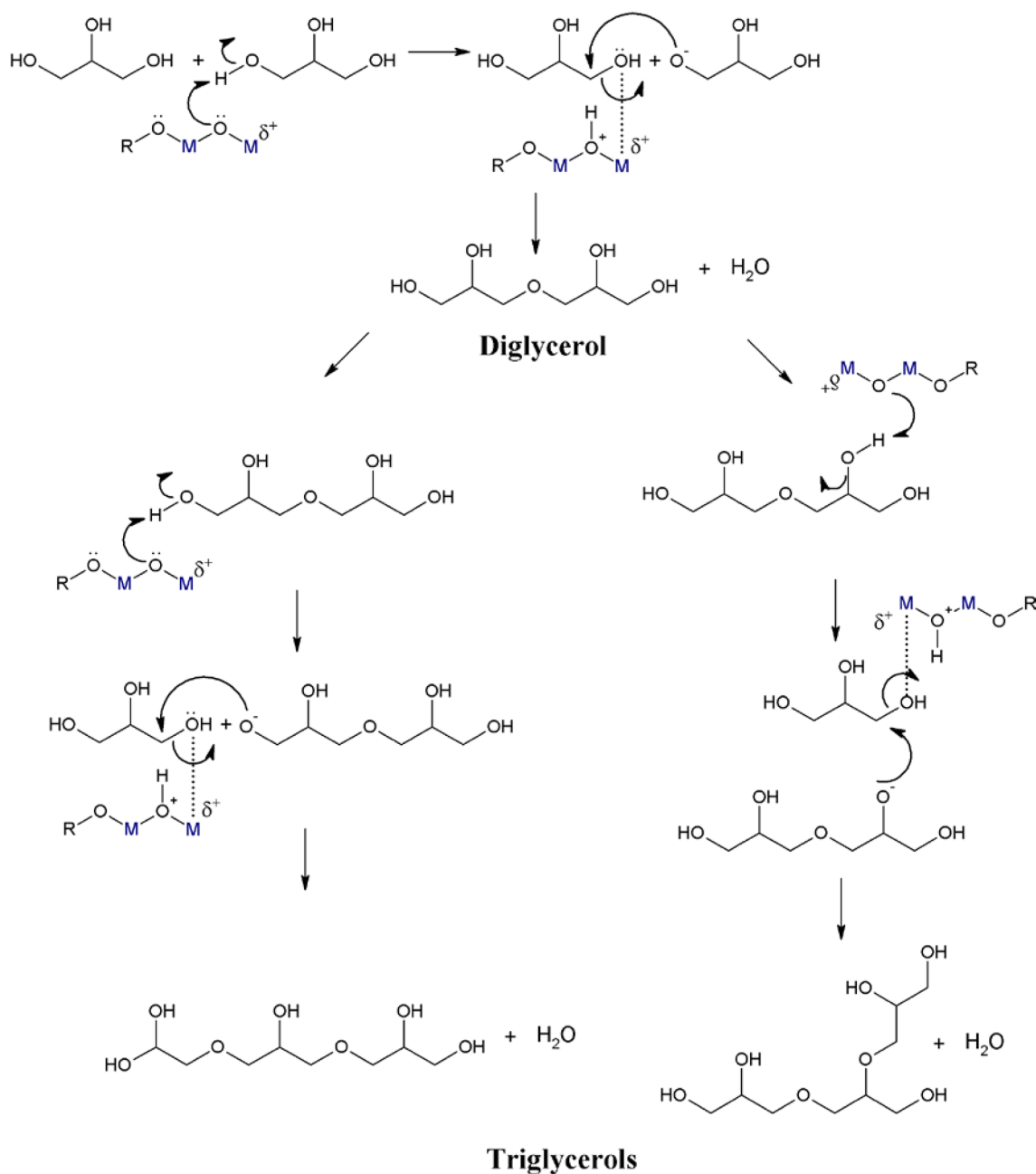
In which CaCO<sub>3</sub> had lower activity than MgO and CaO, due to lack of solubility and basicity [42]. According to Salehpour et al. [43], for the calcium carbonate catalysis, the reaction can proceed by the same mechanism as the calcium hydroxide but it would start differently. The carbonate can deprotonate the primary hydroxyl of the glycerol. The bicarbonate ion generated from the first reaction would quickly decompose into carbon dioxide and hydroxide at elevated temperatures. Thus, the carbonate is not recovered and the reaction is actually catalyzed by calcium hydroxide.

The influence of this remaining CaCO<sub>3</sub> present on CD in the catalytic activity could be considered negligible, due to solubility.

The higher catalytic conversion in the etherification reaction of the calcined material is associated with the thermal treatment of dolomite. Due to the structure of dolomite, the basic properties are originated from the calcination, probably ND shows negligible basic sites. This process provokes the increasing of textural properties (specially  $S_{BET}$ , which is 30 times higher than ND) removes carbonate species and also acts forming alkaline-earth mixed oxides (CaO–MgO), which are the active phases. In this sense, Ruppert et al. have pointed out that the glycerol conversion increases with the amount of basic sites as well as the strength of Lewis acid centers, which facilitate the removal of hydroxyl groups by the presence of  $O^{2-}-M^{n+}$  acid-base pairs, as was indicated for CaO-based catalysts [26]. TPD–CO<sub>2</sub> data, reported in Fig. 6, showed that CaO–MgO system displays strong basic sites that are the active sites in the etherification reaction, which are in agreement with that reported in the literature [17, 26, 27, 44, 45]. Previously, Ruppert et al. [26] have proposed a mechanism in the glycerol etherification where Lewis acid sites (metal oxide coordinates unsaturated metal cations) and Lewis basic sites (oxygen anions) are involved (Scheme 1). These authors established that a basic site attacks a hydroxyl group of a glycerol molecule, extracting a proton. On the other hand, an unsaturated metal site located on the surface of the alkaline earth oxide is able to activate a hydroxyl group of another glycerol molecule, which is attacked by the nucleophilic oxygen obtained in the first step, leading to a diglycerol molecule. The further formation of triglycerol and heavier polymers are consecutive reactions.

### Effects of Reaction Temperature

After confirming that calcined dolomite exhibits the highest activity in the synthesis of polyglycerols in comparison to



**Scheme 1** Mechanism proposed by the glycerol etherification, according to Ruppert et al. (2012)

432 the as-received dolomite, the influence of the reaction temperature was ranged between 200 and 245 °C, maintaining  
 433 constant the catalyst loading on 2 wt% and 24 h of time of stream (Fig. 8).  
 434  
 435

436 Even with a longer reaction time, at the lowest temperature (200 °C), CD exhibited a lower glycerol conversion,  
 437 only 9%; although good selectivity to diglycerol, close to 50%. The increase of the temperature caused a clear increase  
 438 in the conversion, obtaining a glycerol conversion of 77%, maintaining high selectivity towards to diglycerol, nearly  
 439  
 440  
 441

51%, which leads to higher diglycerol yield to that obtained  
 by Barros et al. under similar reaction conditions ( $X_{\text{gly}} = 85\%$   
 $S_{\text{di}} = 40\%$ ), using CaO as active phase coming from eggshell  
 [17].

When the temperature is raised to 245 °C, although the  
 catalyst showed high glycerol conversion, a decrease on  
 diglycerol selectivity was observed ( $X_{\text{gly}} = 91\%$   $S_{\text{di}} = 23\%$   
 and  $S_{\text{tri}} = 22\%$ ). Another important feature highlighted on  
 Fig. 9 is that color and viscosity of obtained products were  
 directly related with the reaction temperature. Thus, a very

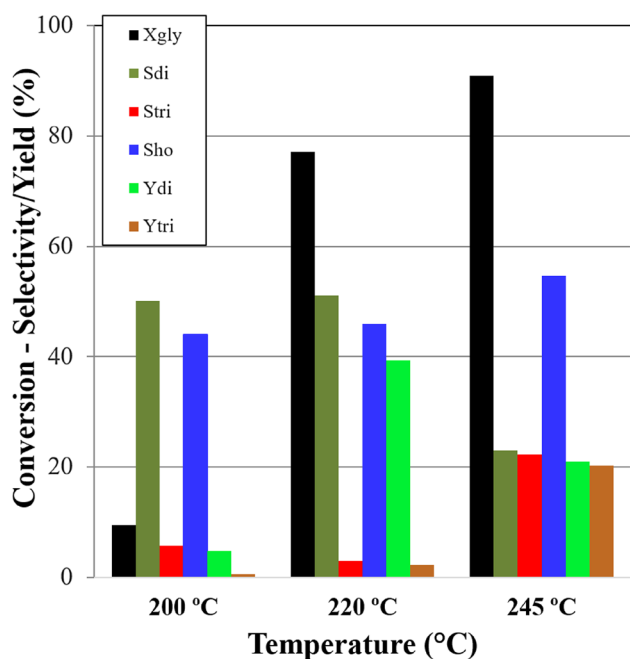


**Fig. 8** Influence of the reaction temperature in the glycerol etherification. (Reaction conditions: 2 wt% of calcined dolomite, 24 h). Glycerol conversion ( $X_{gly}$ ), diglycerol selectivity ( $S_{di}$ ), triglycerol selectivity ( $S_{tri}$ ), high oligomers and other products ( $S_{ho}$ ), diglycerol yield ( $Y_{di}$ ) and triglycerol yield ( $Y_{tri}$ )

clear product, similar to the unreacted glycerol was obtained at 200 °C; while the product obtained at 245 °C was darker and very viscous.

At higher temperature, the polymerization of glycerol increases, with the appearance of oligomers greater than tetraglycerol. The separation of the oligoglycerol mixtures into their components is difficult by direct distillation [20]. Therefore, lower temperature conditions allow the synthesis of the desired products (di- and triglycerol) and it would involve fewer separation steps for the purification of the final product. The content of the glycerol oligomer mixture is regulated by specific laws, according to the European Community legislations, for example, polyglycerol polyricinoleate, used as food additive, was considered, the content of di-, tri- and tetraglycerol should be predominated (not

less than 75%), whereas the amounts of polyglycerols equal to or greater than heptaglycerol should not be greater than 10% [12, 46].

### Evaluation of Catalyst Loading

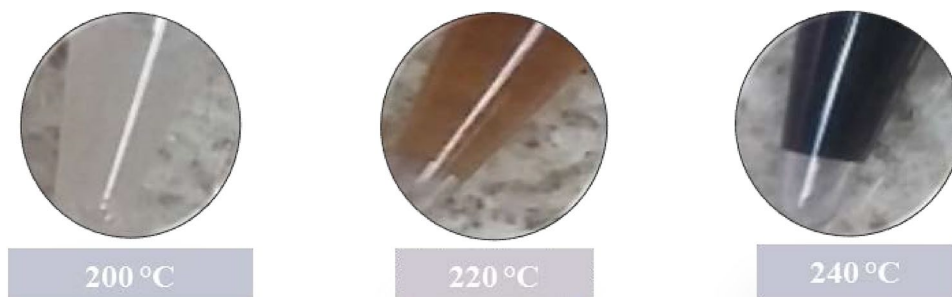
Since reaction temperature of 220 °C led to more diglycerol selectivity and lower formation of higher oligomers and other products, this temperature was used for the catalyst loading evaluation. A trend of increasing the conversion with increasing of catalyst loading (Fig. 10) is observed, reaching 77%  $X_{gly}$  for CD, with  $Y_{di}$  ca. 40% and ca. 2% for  $Y_{tri}$ . For this maximum catalyst loading, calcined eggshell (mainly composed by CaO) led to higher glycerol conversion (85%), but slightly lower  $Y_{di}$  (34%), probably due to diglycerol oligomerization [17].

These data are in agreement with those reported in the literature, where the catalytic activity using basic catalysts and mainly alkaline-earth oxides increases directly with the catalyst loading, obtaining the maximum value for 2 wt% [20, 45]. The use of a higher loading caused a decrease of the glycerol conversion, probably due to the back-scissions of diglycerol to glycerol [20].

In addition, it is also noteworthy that the selective pattern is similar in all cases so an increase in catalyst loading only causes an improvement in catalytic activity by an increase in available active centers, while the selectivity pattern must be attributed to the reaction temperature. The increase of the glycerol conversion with the catalyst loading together with the similar values in the selectivity pattern leads to a diglycerol yield of 40%, while the triglycerol yield is only of 2%. These values are slightly higher to those exposed by Barros et al. [17] for the calcined eggshell thermally treated, where a glycerol conversion of 85% was obtained with a diglycerol yield slightly lower (34%) to that shown for the calcined dolomite.

These temperature and catalyst load conditions are interesting in comparison with previously published results. Using MgAl mixed oxides as base catalysts for glycerol etherification, Garcia-Sancho et al. [15], working at same temperature (220 °C) found a highest conversion of 50.7% for a catalyst loading of 2 wt%. Pouilloux et al. [47] studied

**Fig. 9** Obtained product after the reaction at 200, 220 and 245 °C for 24 h with 2 wt% of calcined dolomite



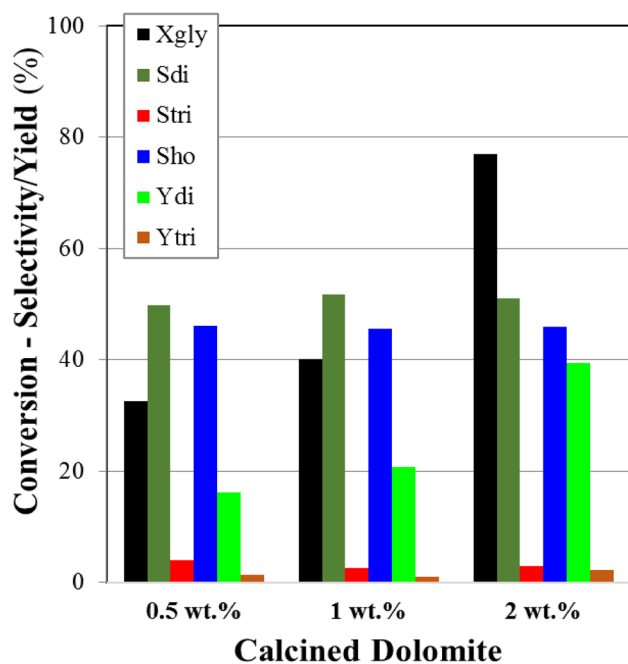


**Fig. 10** Effect of catalyst loading in the glycerol etherification. (Reaction conditions: 220 °C and 24 h). Glycerol conversion ( $X_{Gly}$ ), diglycerol selectivity ( $S_{di}$ ), triglycerol selectivity ( $S_{tri}$ ), high oligomers and other products ( $S_{ho}$ ), diglycerol yield ( $Y_{di}$ ) and triglycerol yield ( $Y_{tri}$ )

507 this reaction with Cesium catalysts impregnated in MCM-41  
 508 and SBA-15, using 1% catalyst, 260 °C, and 24 h of reaction,  
 509 obtaining glycerol conversions of 72% for Cs/SBA15  
 510 and 74% for Cs/MCM-41. For 2 wt% of calcined dolomite,  
 511 a much more cheap material, similar  $X_{gly}$  was obtained at a  
 512 temperature 40 °C lower.

### 513 Effect of Reaction Time

514 Once the parameters of the glycerol etherification have been  
 515 optimized (100 g of glycerol, 2 wt% of calcined dolomite,  
 516 220 °C and 24 h), the influence of the reaction time was  
 517 studied (Fig. 11). It has been observed that the glycerol  
 518 conversion as well as the di- and triglycerol yield increase with  
 519 the reaction time. In the first hours, it is observed that the  
 520 glycerol conversion is lower, only 8% after 6 h of reaction  
 521 time. This fact could indicate that it is necessary an activa-  
 522 tion step to accelerate the glycerol etherification since a con-  
 523 version close to 80% is obtained after a reaction time of 24 h.  
 524 Considering the mechanism proposed by previous authors,  
 525 the glycerol etherification takes place in two steps [26, 44].  
 526 In a first step, a basic site extracts a proton of the glycerol  
 527 molecule, while in a second step, an unsaturated site favors  
 528 the attack of the deprotonated glycerol to another glycerol  
 529 molecule (Scheme 1). From the obtained data in Fig. 11,  
 530 it can be inferred that the formation of the deprotonated

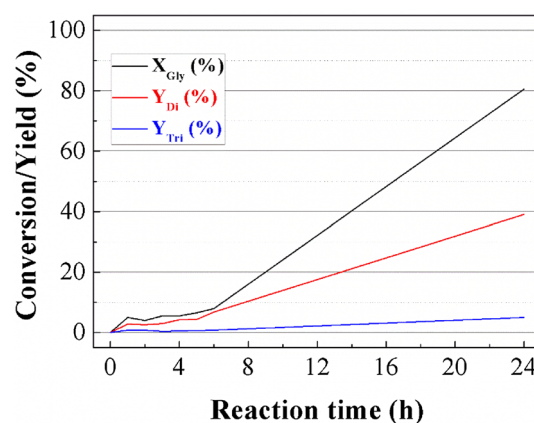


**Fig. 11** Kinetic study in the glycerol etherification. (Reaction conditions: 2 wt% of calcined dolomite, 220 °C). Glycerol conversion ( $X_{Gly}$ ), diglycerol yield ( $Y_{di}$ ) and triglycerol yield ( $Y_{tri}$ )

glycerol species could be limited requiring higher reaction  
 531 temperature or higher reaction time than the second step. 532

The catalytic data also show how diglycerol is formed  
 533 at shorter reaction times in comparison to triglycerol mol- 534  
 ecules. Later, from diglycerol molecules can be obtained 535  
 triglycerol molecules or polyglycerols with higher chain fol- 536  
 lowing the same mechanism shown in Scheme 1 [26]. The 537  
 increase of the polyglycerol chain is in agreement with the 538  
 literature, where the use of prolonged reaction time favors 539  
 the condensation of higher proportion of glycerol molecules 540  
 or other side reactions. In the present study, the use of rela- 541  
 tively low temperature (220 °C) limits the existence of unde- 542  
 sired side reactions, which can generate toxic products such 543  
 as acrolein or glycidol [19, 27, 48]. 544

### 545 Reusability and Stability

The use of inexpensive and reusable catalysts is key to obtain  
 546 sustainable and competitive catalysts. For this purpose, the  
 547 product mixture (reaction with 2 wt% of dolomite, 24 h at  
 548 220 °C) and catalyst was separated by decantation. In order  
 549 to maintain a similar catalyst loading, the glycerol-catalyst  
 550 weight ratio was maintained. The catalytic data (Fig. 12)  
 551 show a decrease of the glycerol conversion from 80 to 35%  
 552 after the first reuse and 40% after second reuse, indicat-  
 553 ing that the conversion is more or less constant after the  
 554 first cycle. Regarding the selectivity, all reactions maintain  
 555 approximately the same pattern, confirming that selectivity  
 556 is directly related with the reaction temperature. 557

The decay of glycerol conversion could be assigned to  
 558 several factors. It is difficult to know if the Mg and Ca spe-  
 559 cies detected by ICP (Table 2) come from the partial leach-  
 560 ing of the calcined dolomite or can be attributed to the loss  
 561 of small particle in the filtration step since the obtained prod-  
 562 uct has high density. Previous researches have established 563

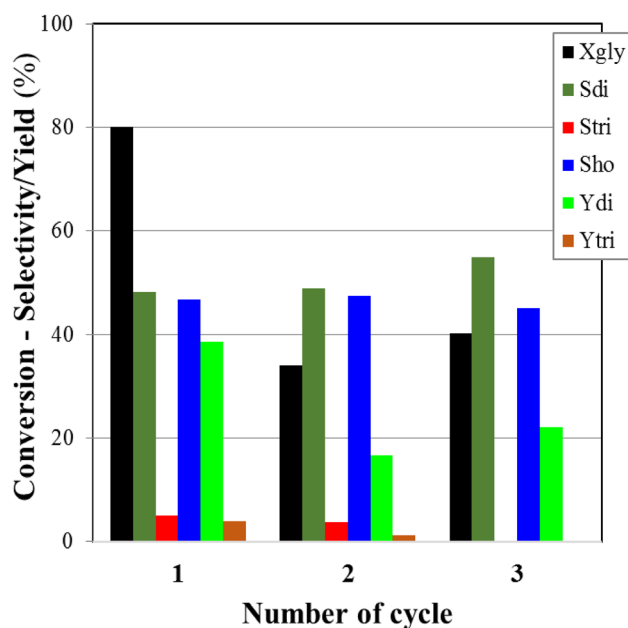


**Fig. 12** Reuse tests (calcined dolomite, 2 wt%, 220 °C and 24 h) (filtration between each cycle)

**Table 2** Ca and Mg amounts determined by ICP-OES on reaction mixture obtained with 2 wt% of commercial CaO, 2 wt% CD (220 °C, and 24 h of reaction) and from reusability tests

Sample	Concentration (g/L)	
	Ca	Mg
Glycerol (reactant)	–	–
Commercial CaO	13.68 ± 0.364	–
220 °C, 2% CD	7.03 ± 0.09	0.19 ± 0.01
First run	9.97 ± 0.05	0.16 ± 0.01
Second run	1.78 ± 0.24	0.19 ± 0.004
Third run	0.85 ± 0.02	0.24 ± 0.03

CD calcined dolomite

the loss of  $\text{Ca}^{2+}$  species [16, 23, 40] or  $\text{Cs}^+$  species in the glycerol etherification, which suggests that the reaction could be partially homogeneous [47]. Previous studies have pointed out that the homogeneous contribution is related to the formation of a calcium glyceroxide phase that exhibits high activity in basic reactions such as glycerol etherification [26] or synthesis of biodiesel [49, 50].

Table 2 shows the leaching of calcium and magnesium for CD catalyst after different catalytic cycles and compared with commercial CaO. It has been remarked that the  $\text{Ca}^{2+}$  leached from CD tests was much lower than that observed with commercial CaO (test performed on our previous study) even though the test with CD was performed up to 24 h. Considering dolomite composition, determined by XRF, and that 2 g of catalyst were used in each test for

100 g of glycerol (density:  $1.26 \text{ g mL}^{-1}$ ), there would be initially  $20.41 \text{ g L}^{-1}$  of Ca and  $4.03 \text{ g L}^{-1}$  of Mg, considering that  $\text{Ca}^{2+}$  and  $\text{Mg}^{2+}$  were completely leached to glycerol. Therefore, analyzing the remaining metal amounts in the products, it can be noticed that for the first run, both calcium and magnesium leaching was of 49% and 4%, respectively. Considering the decreasing on metal content on the catalyst due to leaching, for second run Ca leaching is of 17% and 5% for Mg; and finally for third run, 10% Ca and 7% Mg. These data confirm that the decrease on glycerol conversion is due to the lower amount of basic sites remaining on the catalyst, being the most active site those related to calcium species.

Calcined dolomite was previously used as solid basic catalyst in the synthesis of biodiesel. Several authors have reported that the complete recovery of the active phase was not possible by the partial leaching of  $\text{Ca}^{2+}$  and  $\text{Mg}^{2+}$  species, although this leaching did not cause a pronounced decrease of the fatty acid methyl ester (FAME) yield [32, 44, 51]. Jaiyen et al. [52] evaluate dolomite and waste seashell as catalysts for methanolysis of palm oil to biodiesel observing that the calcined dolomite was more tolerant to deactivation than calcined seashells by the reaction of CaO active phase with glycerol to form  $\text{Ca}(\text{C}_3\text{H}_7\text{O}_3)_2$ .

For other base catalyzed reactions, such as aldol-condensation of furfural with acetone, the catalyst derived from dolomite also presented leaching processes, although the deactivation was very low and attributed to the formation of carbonaceous deposits [53]. The synthesis of glycerol carbonate from glycerol and dimethylcarbonate also revealed a decline of the catalytic activity after several cycles by a progressive loss of the CaO–MgO phases [33]. Galadima and Muraza [54] summarized a series of works on glycerol carbonate production and associated resistancy to deactivation with mass transfer properties. Catalysts with poor mass transfer properties were subject to quick deactivation with time.

Other cause of the loss of the activity can be ascribed to the alkaline earth mixed oxides (CaO–MgO) obtained from the thermal treatment of the raw dolomite that have high susceptibility to retain  $\text{CO}_2$  molecules, causing a superficial carbonation and therefore the loss of the available basic sites provoking a decrease of the catalytic activity. Thus, Ilgen et al. [51] regenerated the active phase by calcination to remove the carbonate species and the carbonaceous deposits formed on the surface for the synthesis of biodiesel. Nonetheless, the FAME yield decreased in comparison to the first run.

For the second set of reusability tests (Fig. 13), after the first cycle (reaction at 220 °C, 2% CD and 24 h) after dissolution in ultrapure water followed by filtration, the catalyst was calcined at 800 °C and 2 h, moreover, the amount of glycerol was adjusted to maintain the catalyst/glycerol ratio.

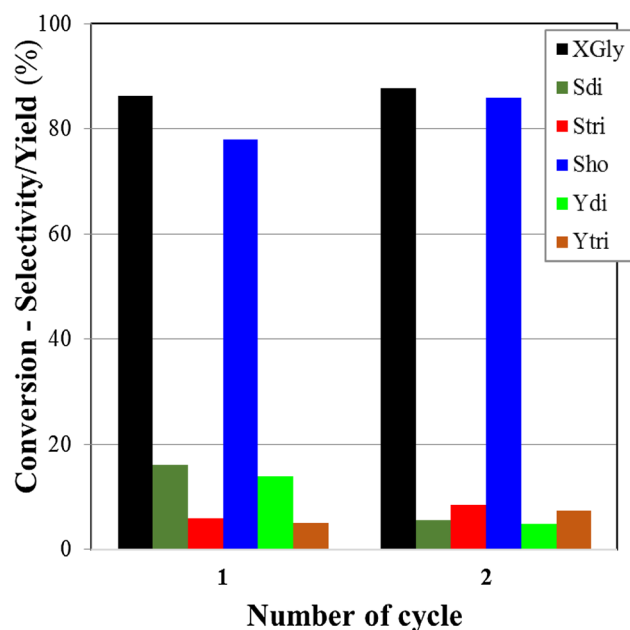


**Fig. 13** Reuse tests (calcined dolomite, 2 wt%, 220 °C and 24 h) (calcination at 800 °C for 2 h before new cycle)

631 Despite similar glycerol conversions (86% on first run  
632 and 88% on second run), there was a drop on diglycerol  
633 selectivity, reaching half of the previous value, and a slightly  
634 increase on triglycerol selectivity (from 6 to 8%). Catalyst  
635 from second run could not be separated from the mixture  
636 to run another cycle, pointing to a considerable dissolution  
637 on the reaction medium, what could have contributed to the  
638 similar conversion and the differences on oligoglycerols  
639 yields.

640 The first set of reusability tests (Fig. 12) presented a  
641 drop on conversion after the first cycle, however kept similar  
642 selectivity. On the other hand, the second set of tests  
643 (Fig. 13) had a lower yield due to the drop on selectivity.  
644 Washing the catalyst with water probably changed the cata-  
645 lyst, being very likely that the surface was hydroxylated,  
646 modifying the catalytic properties. The washing step elimi-  
647 nated the adsorbed glycerol or oligomers and hot spots  
648 during the calcination were avoided. However, the thermal  
649 process also reduced the amount of material and probably  
650 consumed active species such as calcium glyceroxide,  
651 decreasing its selectivity to the oligomers. Therefore, the first  
652 procedure for catalyst reusability is more interesting since it  
653 leads to more cycles and diglycerol yielding.

## 654 Conclusions

655 Dolomite was used as catalytic precursor to obtain a cata-  
656 lytic system (MgO–CaO) for the glycerol etherification. The  
657 characterization data reported that it is necessary 800 °C to

658 convert dolomite in MgO–CaO. The thermal treatment is an  
659 exothermic process, which causes a decrease of the particle  
660 size and an increase of the specific surface area. The TPD-  
661 CO<sub>2</sub> experiment reported that the obtained sample displays  
662 basic sites with great strength.

663 For the parameters covered on this study, calcined dolo-  
664omite features lead to the following set of best conditions:  
665 catalyst load of 2%, temperature of 220 °C and 24 h of reac-  
666 tion time. Under these conditions, there was glycerol conver-  
667 sion of 77%, and di and triglycerol selectivities of 51% and  
668 3%, respectively.

669 The influence of reaction time reveals that the reaction is  
670 slow along the first hours and later the reaction rate increases  
671 probably due to the first etherification step being thermody-  
672 namically or kinetically limited.

673 Reusability and stability tests showed loss of catalytic  
674 activity from the first reuse, as well as significant differences  
675 in the selectivity to the diglycerol due to active phase leach-  
676 ing to the reaction mixture, suggesting some homogeneous  
677 contribution.

678 Calcined dolomite catalytic performance allows us to  
679 conclude that it has potential to be used on glycerol oli-  
680 gomerization, reaching significant glycerol conversions  
681 when used in smaller amounts and temperatures than those  
682 previously reported on other reaction routes. Dolomites  
683 application as catalyst on glycerol oligomerization is prom-  
684 ising considering that this material has low price, reusability  
685 capacity and large availability world widely.

686 **Acknowledgements** This work was supported by CNPq (Conselho  
687 Nacional de Desenvolvimento Científico e Tecnológico), Centro de  
688 Tecnologias Estratégicas do Nordeste [INT/MCT-FACEPE APQ-1015-  
689 3.06/14], Central Analítica—[UFC/CT-INFRA/MCTI-SISNANO/  
690 Pró-Equipamentos], CAPES, Project CAPES/FUNCAP (Áreas Estrá-  
691 tégicas) [Project E1-0079-0004301] and FEDER funds and Spanish  
692 Ministry of Economy and Competitiveness [IEDI-2016-00743] I3  
693 program and project [CTQ2015-68951-C3-3-R].

## 694 Compliance with ethical standards

695 **Conflict of interest** The authors declare that they have no conflict of  
696 interest.

## 697 References

- 698 1. Marchetti, J.M., Miguel, V.U., Errazu, A.F.: Possible methods for  
699 biodiesel production. *Renew. Sustain. Energy Rev.* **11**, 1300–1311  
700 (2007)
- 701 2. Anuar, M.R., Abdullah, A.Z., Othman, M.R.: Etherification of  
702 glycerol to polyglycerols over hydrotalcite catalyst prepared using  
703 a combustion method. *Catal. Commun.* **32**, 67–70 (2013)
- 704 3. Behr, A., Eilting, J., Irawadi, K., Leschinski, J., Lindner, F.:  
705 Improved utilisation of renewable resources: new important  
706 derivatives of glycerol. *Green Chem.* **10**, 13–30 (2008)
- 707 4. Gholami, Z., Abdullah, A.Z., Lee, K.-T.: Dealing with the surplus  
708 of glycerol production from biodiesel industry through catalytic

- 709 upgrading to polyglycerols and other value-added products. *Renew. Sustain. Energy Rev.* **39**, 327–341 (2014)
- 710
- 711 5. Ciriminna, R., Pina, C., Rossi, M., Pagliaro, M.: Understanding  
 AQ3 the glycerol market. *Eur. J. Lipid Sci. Technol.* **116**, 1–22 (2014)
- 713 6. Cecília, J.A., García-Sabchez, C., Mérida-Robles, J., Santamaría-  
 714 González, J., Moreno-Tost, R., Maireles-Torres, P.J.: V and V-P  
 715 containing Zr-SBA-15 catalysts for dehydration of glycerol to  
 716 acrolein. *Catal. Today* **254**, 43–52 (2015)
- 717 7. García-sancho, C., Cecilia, J.A., Moreno-Ruiz, A., Mérida-robles,  
 718 J.M., Gonzales, J.S., Moreno-tost, R., Maireles-Torres, P.: Influence  
 719 of the niobium supported species on the catalytic dehydration  
 720 of glycerol to acrolein. *Appl. Catal. B Environ.* **179**, 139–149  
 721 (2015)
- 722 8. Nakagawa, Y., Shinmi, Y., Koso, S., Tomishige, K.: Direct  
 723 hydrogenolysis of glycerol into 1,3-propanediol over rhenium-  
 724 modified iridium catalyst. *J. Catal.* **272**, 191–194 (2010)
- 725 9. Ketchie, W.C., Murayama, M., Davis, R.J.: Selective oxidation  
 726 of glycerol over carbon-supported AuPd catalysts. *J. Catal.* **250**,  
 727 264–273 (2007)
- 728 10. Arcanjo, M.R.A., Silva, I.J., Rodríguez-castellón, E., Infantes-  
 729 molina, A., Vieira, R.S.: Conversion of glycerol into lactic acid  
 730 using Pd or Pt supported on carbon as catalyst. *Catal. Today* **279**,  
 731 317–326 (2017)
- 732 11. Kunkes, E.L., Simonetti, D.A., Dumesic, J.A., Pyrz, W.D., Muri-  
 733 llo, L.E., Chen, J.G., Buttrey, D.J.: The role of rhenium in the  
 734 conversion of glycerol to synthesis gas over carbon supported  
 735 platinum–rhenium catalysts. *J. Catal.* **260**, 164–177 (2008)
- 736 12. Marquez-Alvarez, C., Sastre, E., Pariente, J.: Solid catalysts for  
 737 the synthesis of fatty esters of glycerol, polyglycerols and sorbitol  
 738 from renewable resources. *Top. Catal.* **27**, 105–117 (2004)
- 739 13. Ruppert, A.M., Parvulescu, A.N., Arias, M., Hausoul, P.J.C.,  
 740 Bruijninx, P.C.A., Klein, R.J.M., Weckhuysen, B.M.: Synthesis  
 741 of long alkyl chain ethers through direct etherification of biomass-  
 742 based alcohols with 1-octene over heterogeneous acid catalysts. *J.*  
 743 *Catal.* **268**, 251–259 (2009)
- 744 14. Liu, F., De Oliveira Vigier, K., Pera-Titus, M., Pouilloux, Y., Cla-  
 745 cencs, J.M., Decampo, F., Jérôme, F.: Catalytic etherification of  
 746 glycerol with short chain alkyl alcohols in the presence of Lewis  
 747 acids. *Green Chem.* **15**, 901 (2013)
- 748 15. García-sancho, C., Moreno-tost, R., Mérida-robles, J.M., San-  
 749 tamaría-gonzález, J., Jiménez-lópez, A., Torres, P.M.: Etherifica-  
 750 tion of glycerol to polyglycerols over MgAl mixed oxides. *Catal.*  
 751 *Today* **167**, 84–90 (2009)
- 752 16. Moreno-Tost, R., Guerrero-Urbaneja, P., García-Sancho, C.,  
 753 Mérida-Robles, J., Santamaría-González, J., Jiménez-López, A.,  
 754 Maireles-Torres, P.: Glycerol valorization by etherification to  
 755 polyglycerols by using metal oxides derived from MgFe hydro-  
 756 talcites. *Appl. Catal. A Gen* **470**, 199–207 (2014)
- 757 17. Barros, F.J.S., Moreno-tost, R., Cecilia, J.A., Ledesma-Muñoz,  
 758 A.L., De Oliveira, L.C.C., Luna, F.M.T., Vieira, R.S.: Glycerol  
 759 oligomers production by etherification using calcined eggshell as  
 760 catalyst. *Mol. Catal.* **433**, 282–290 (2017)
- 761 18. Sivaiah, M.V., Robles-Manuel, S., Valange, S., Barrault, J.: Recent  
 762 developments in acid and base-catalyzed etherification of glycerol  
 763 to polyglycerols. *Catal. Today* **198**, 305–313 (2012)
- 764 19. Sutter, M., Da Silva, E., Duguet, N., Raoul, Y., Métay, E., Lemaire,  
 765 M.: Glycerol ether synthesis: a bench test for green chemistry con-  
 766 cepts and technologies. *Chem. Rev.* **115**, 8609–8651 (2015)
- 767 20. Martin, A., Richter, M.: Oligomerization of glycerol—a critical  
 768 review. *Eur. J. Lipid Sci. Technol.* **113**, 100–117 (2011)
- 769 21. Plasman, V., Caulier, T., Boulos, N.: Polyglycerol esters demon-  
 770 strate superior antifogging properties for films. *Plast. Addit.*  
 771 *Compd.* **7**, 30–33 (2005)
- 772 22. Medeiros, M.D.A., Rezende, J.D.C., Araújo, M.H., Lago, R.M.:  
 773 Influência da Temperatura e da Natureza do Catalisador na  
 774 Polimerização do Glicerol (Influence of temperature and nature of  
 the catalyst on glycerol polymerization). *Polímeros* **20**, 188–193  
 (2010)
- 775
- 776 23. Richter, M., Krisnandi, Y.K., Eckelt, R., Martin, A.: Homogene-  
 777 ously catalyzed batch reactor glycerol etherification by CsHCO<sub>3</sub>.  
 778 *Catal. Commun.* **9**, 2112–2116 (2008)
- 779 24. Eshuis, J.I., Laan, J.A., Potman, R.P.: Polymerization of glycerol  
 780 using a zeolite catalyst. US Patent 5635588 (1997)
- 781 25. Cottin, K., Clacens, J.-M., Pouilloux, Y., Barrault, J.: Préparation  
 782 de diglycérol et triglycérol par polymérisation directe du glycérol  
 783 en présence de catalyseurs solides. *Oléagineux Corps Gras Lipi-*  
 784 *des.* **5**, 405–412 (1998)
- 785 26. Ruppert, A.M., Meeldijk, J.D., Kuipers, B.W.M., Ernø, B.H.,  
 786 Weckhuysen, B.M.: Glycerol etherification over highly active  
 787 CaO-based materials: new mechanistic aspects and related col-  
 788 loidal particle formation. *Chem. Eur. J.* **14**, 2016–2024 (2008)
- 789 27. Clacens, J., Pouilloux, Y., Barrault, J.: Selective etherification of  
 790 glycerol to polyglycerols over impregnated basic MCM-41 type  
 791 mesoporous catalysts. *Appl. Catal. A Gen* **227**, 181–190 (2002)
- 792 28. Pérez-Barrado, E., Pujol, M.C., Aguiló, M., Llorca, J., Cesteros,  
 793 Y., Díaz, F., Pallarès, J., Marsal, L.F., Salagre, P.: Influence of  
 794 acid–base properties of calcined MgAl and CaAl layered double  
 795 hydroxides on the catalytic glycerol etherification to short-chain  
 796 polyglycerols. *Chem. Eng. J.* **264**, 547–556 (2015)
- 797 29. Shahraki, B.K., Mehrabi, B., Dabiri, R.: Thermal behavior of  
 798 Zefreh dolomite mine (Central Iran). *J. Min. Metall. Sect. B Met-*  
 799 *all.* **45**, 35–44 (2009)
- 800 30. Wilson, K., Hardacre, C., Lee, A.F., Montero, J.M., Shellard, L.:  
 801 The application of calcined natural dolomitic rock as a solid base  
 802 catalyst in triglyceride transesterification for biodiesel synthesis.  
 803 *Green Chem.* **10**, 654–659 (2008)
- 804 31. Ngamcharussrivichai, C., Nunthasanti, P., Tanachai, S., Buny-  
 805 kiatt, K.: Biodiesel production through transesterification over  
 806 natural calciums. *Fuel Process. Technol.* **91**, 1409–1415 (2010)
- 807 32. Correia, L.M., de Sousa, N., Novaes, D.S., Cavalcante Jr, C.L.,  
 808 Cecilia, J.A., Rodríguez-castellón, E., Silveira, R.: Characteriza-  
 809 tion and application of dolomite as catalytic precursor for canola  
 810 and sunflower oils for biodiesel production. *Chem. Eng. J.* **269**,  
 811 35–43 (2015)
- 812 33. Algoufi, Y.T., Kabir, G., Hameed, B.H.: Synthesis of glycerol car-  
 813 bonate from biodiesel by-product glycerol over calcined dolomite.  
 814 *J. Taiwan Inst. Chem. Eng.* **70**, 179–187 (2017)
- 815 34. Elbaba, I.F., Williams, P.T.: High yield hydrogen from the pyroly-  
 816 sis–catalytic gasification of waste tyres with a nickel/dolomite  
 817 catalyst. *Fuel.* **106**, 528–536 (2013)
- 818 35. Engler, P., Santana, M.W., Mittleman, M.L.: Non-isothermal  
 819 in situ XRD analysis of dolomite decomposition. *Rigaku J.* **5**,  
 820 3–8 (1988)
- 821 36. Gunasekaran, S., Anbalagan, G.: Thermal decomposition of natu-  
 822 ral dolomite. *Bull. Mater. Sci.* **30**, 339–344 (2007)
- 823 37. Granados, M.L., Poves, M.D.Z., Alonso, D.M., Mariscal, R.,  
 824 Galisteo, F.C., Moreno-Tost, R., Santamaría, J., Fierro, J.L.G.:  
 825 Biodiesel from sunflower oil by using activated calcium oxide.  
 826 *Appl. Catal. B Environ.* **73**, 317–326 (2007)
- 827 38. Thommes, M., Kaneko, K., Neimark, A.V., Olivier, J.P., Rodrig-  
 828 uez-reinoso, F., Rouquerol, J., Sing, K.S.W.: Physisorption of  
 829 gases, with special reference to the evaluation of surface area and  
 830 pore size distribution (IUPAC technical report). *Pure Appl. Chem.*  
 831 **87**, 1051–1069 (2015)
- 832 39. Ávila, I., Crnkovic, P.M., Milioli, F.E.: Metodologia para o estudo  
 833 da porosidade de dolomita em ensaio de sulfatação interrompida.  
 834 *Quim. Nova* **33**, 1732–1738 (2010)
- 835 40. Wang, R., Li, H., Chang, F., Luo, J., Hanna, M.A., Tan, D., Hu,  
 836 D., Zhang, Y., Song, Y., Song, B.: A facile, low-cost route for  
 837 the preparation of calcined porous calcite and dolomite and their  
 838 application as heterogeneous catalysts in biodiesel production.  
 839 *Catal. Sci. Technol.* **3**, 2244–2251 (2013)
- 840

- 841 41. Santos, R.C.R., Vieira, R.B., Valentini, A.: Optimization study  
842 in biodiesel production via response surface methodology using  
843 dolomite as a heterogeneous catalyst. *J. Catal.* **2014**, 1–11 (2014)  
844 42. Garti, N., Aserin, A., Zaidman, B.: Polyglycerol esters: optimi-  
845 zation and techno-economic evaluation. *J. Am. Oil Chem. Soc.*  
846 **1981**, 878–883 (1981)  
847 43. Salehpour, S., Dube, M.A.: Towards the sustainable production  
848 of higher-molecular-weight polyglycerol. *Macromol. Chem. Phys.*  
849 **212**, 1284–1293 (2011)  
850 44. Calatayud, M., Ruppert, A.M., Weckhuysen, B.M.: Theoreti-  
851 cal study on the role of surface basicity and lewis acidity on the  
852 etherification of glycerol over alkaline earth metal oxides. *Chem.*  
853 *Eur. J.* **116**, 10864–10870 (2009)  
854 45. Gholami, Z., Abdullah, A.Z., Lee, K.T.: Catalytic etherification  
855 of glycerol to diglycerol over heterogeneous calcium-based mixed  
856 oxide catalyst: reusability and stability. *Chem. Eng. Commun.*  
857 **202**, 1397–1405 (2015)  
858 46. European Parliament: and Council Directive No. 95/2/EC (1995)  
859 47. Pouilloux, Y., Ramirez, A.E., Clacens, J., Lorentz, C.: Comparison  
860 between SBA-15 and MCM-41 structure on the stability and the  
861 selectivity of basic catalysts in oligomerization of glycerol. *Curr.*  
862 *Org. Chem.* **16**, 2774–2781 (2012)
48. Ayoub, M., Khayoon, M.S., Abdullah, A.Z.: Synthesis of oxygen-  
ated fuel additives via the solventless etherification of glycerol. *Bioresour. Technol.* **112**, 308–312 (2012)
49. Kouzu, M., Tsunomori, M., Yamanaka, S., Hidaka, J.: Solid base  
catalysis of calcium oxide for a reaction to convert vegetable oil  
into biodiesel. *Adv. Powder Technol.* **21**, 488–494 (2010)
50. León-Reina, L., Cabeza, A., Rius, J., Maireles-Torres, P., Alba-  
Rubio, A.C., López Granados, M.: Structural and surface study  
of calcium glyceroxide, an active phase for biodiesel production  
under heterogeneous catalysis. *J. Catal.* **300**, 30–36 (2013)
51. Ilgen, O.: Dolomite as a heterogeneous catalyst for transesterifica-  
tion of canola oil. *Fuel Process. Technol.* **92**, 452–455 (2011)
52. Jaiyen, S., Naree, T., Ngamcharussrivichai, C.: Comparative study  
of natural dolomitic rock and waste mixed seashells as heterogene-  
ous catalysts for the methanolysis of palm oil to biodiesel. *Renew.*  
*Energy.* **74**, 433–440 (2015)
53. O'Neill, R.E., Vanoye, L., De Bellefon, C., Aiouache, F.: Aldol-  
condensation of furfural by activated dolomite catalyst. *Appl.*  
*Catal. B Environ.* **144**, 46–56 (2014)
54. Galadima, A., Muraza, O.: Sustainable production of glycerol  
carbonate from by-product in biodiesel plant. *Waste Biomass*  
*Valorization* **8**, 141–152 (2017)

## Affiliations

Fernando José S. Barros<sup>1</sup> · Juan A. Cecilia<sup>2</sup> · Ramón Moreno-Tost<sup>2</sup> · Matheus F. de Oliveira<sup>1</sup> ·  
Enrique Rodríguez-Castellón<sup>2</sup> · Francisco Murilo T. Luna<sup>1</sup> · Rodrigo S. Vieira<sup>1</sup> 

<sup>1</sup> Grupo de Pesquisa em Separações por Adsorção–GPSA, Departamento de Engenharia Química, Universidade Federal do Ceará, Campus do Pici, 709, Fortaleza, CE 60.455-760, Brazil

<sup>2</sup> Facultad de Ciencias, Departamento de Química Inorgánica, Mineralogía y Cristalografía (Unidad Asociada ICP-CSIC), Universidad de Málaga, Campus de Teatinos s/n, 29071 Malaga, Spain